

PAPER • OPEN ACCESS

Conjugate mixed convection with discrete heat sources in a rectangular channel with surface radiation

To cite this article: N K Chaurasia *et al* 2016 *J. Phys.: Conf. Ser.* **745** 032031

View the [article online](#) for updates and enhancements.

Related content

- [Numerical investigation of natural and mixed convection heat transfer on optimal distribution of discrete heat sources mounted on a substrate](#)
M V Karvinkoppa and T K Hotta
- [Current, voltage and temperature distribution modeling of light-emitting diodes based on electrical and thermal circuit analysis](#)
J Yun, J-I Shim and D-S Shin
- [Constant-flux discrete heating in a unit aspect-ratio annulus](#)
J M Lopez, M Sankar and Younghae Do



IOP | ebooks™

Bringing together innovative digital publishing with leading authors from the global scientific community.

Start exploring the collection—download the first chapter of every title for free.

Conjugate mixed convection with discrete heat sources in a rectangular channel with surface radiation

N K Chaurasia¹, S Gedupudi² and S P Venkateshan³

Heat Transfer and Thermal Power laboratory
Department of Mechanical Engineering
Indian institute of technology madras, Chennai, India

E-mail: nitish020990@gmail.com¹, sateeshg@iitm.ac.in², spv@iitm.ac.in³

Abstract. Mixed convection is seen in high power devices where natural convection alone is not enough. At high temperatures radiation also contributes considerably. This work is concerned with the effect of surface radiation on mixed convection and conjugate convection in a channel with discrete heat sources. Flow is laminar and the parameters considered for this study are thermal conductivity of PCB (printed circuit board), Reynolds number, position of heat sources and emissivity of surface (emissivity of the inner surfaces of the channel are kept constant while those of the heat sources is varied). Constant fluid properties with $Pr = 0.707$ with Boussinesq approximation is considered. All numerical simulation has been done using FLUENT. The Reynolds number ranges from 115 to 690 (corresponding to air inlet velocity 0.25 to 1.5m/sec) and emissivity ranges from 0.1 to 0.9. Temperatures of heat sources decrease with increase in velocity, thermal conductivity of PCB and the emissivity.

1. Introduction

When natural convection alone is not enough to dissipate all the necessary heat generated, mixed convection or forced convection is used. At temperatures typical of electronic components 85° C, radiation contributes considerably. With advances in technology components keep decreasing in size and hence need to dissipate larger and larger amounts of heat from the given surface area. For reliable operation appropriate cooling is required. Such type of problem occurs in electronic components cooling, nuclear reactors technology, heat exchangers etc.

Hotta et al. [1] conducted steady state experiments with five discrete heat sources (non-identical) under mixed convection cooling and found that the maximum temperature decreases with increase in the value of λ (heuristic non-dimensional geometric distance parameter) and the optimal configuration occurs for the highest value of λ . Premachandran and Balaji [2] performed numerical study of a 2-D rectangular channel with protruding heat sources, by fixing the size of channel, thickness of heat sources and substrate and spacing between the heat sources. They studied the effect of Re_s , Gr_s^* , k_p/k_f , k_s/k_f , ϵ_p and ϵ_s . They found that with increase in Re , maximum temperature and effect of radiation decrease. With increase in k_p/k_s and k_s/k_f maximum temperature decreases. Sawant and Gururaja [3] studied conjugate mixed convection with surface radiation from a vertical electronic board with flush mounted heat sources. They studied the effect of modified Richardson number, thermal conductivity and surface emissivity. Yusoff et al. [4] have done experimental as well as numerical study of a rectangular duct in which two PLCC (Plastic leaded chip carriers) are placed in-line, on a printed circuit board and cooled by forced convection. They studied temperature and Nusselt number variations for different powers and spacings of PLCC. They concluded



that the thermal performance increases with increase in inlet velocity and package spacing. Dogan et al. [5] studied mixed convection for arrays of discrete heat sources inside a horizontal channel experimentally. Each of lower and upper surfaces was equipped with 8×4 heat sources and parameters studied were different aspect ratios, Reynolds and Grashof numbers. For small values of aspect ratios, the effect of free convection becomes more important only at high values of Grashof numbers. Also they suggest that a device placed on the top wall will have temperatures much higher than that on bottom wall. They conclude that when dealing with high power densities in horizontal channel flow, heat sources with higher dissipation rates should be placed along the bottom wall. Choi and Kim [6] numerically studied the conjugate 3-D mixed convection in a channel and proposed a modified five percent rule (flow for which a group of non-dimensional variables deviates by more than 5% from the asymptotes for natural convection and forced convection will be treated as a mixed flow) considering maximum non-dimensional temperature and conductivity ratio, Reynolds number and Grashof number. Basak et al. [7] studied the mixed convection and the effect of Grashof number for lid driven flows in a square cavity, with the bottom wall heated uniformly and non-uniformly. For fixed Re and Pr, the strength of circulation is proportional to Gr. As Gr increases, the effect of buoyancy increases leading to an increase in strength of circulation. Heat transfer is mostly by convection for higher values of Pr. Sugavanam et al. [8] conducted numerical investigation of conjugate heat transfer from a thin flush mounted heat sources for a two dimensional steady laminar forced convection for different values of thermal conductivities of substrate. The Nu for the hydrodynamically developing flow situation was found to be much higher compared with the fully developed flow situation at high Re because of predominance of conduction. The effects of the substrate thickness were important only for the conductivity ratio, $k_s/k_f > 10$. Saied and Ghasemi [9] studied numerically mixed convection in a two dimensional horizontal channel for open cavity. For different locations of the constant temperature heat source in the cavity, as the cavity aspect ratio increases, an initial decrease in the average temperature and an increase in the heat transfer rate can be observed for low aspect ratios of the cavity; however this trend stabilizes at higher values of aspect ratios.

From the literature survey, it is found that the effect of surface radiation with conjugate mixed convection for a 3-D channel with protruding discrete heat sources has not been studied in the present study. Hence, a numerical analysis with six volumetric heat generative sources mounted on the lower surface of the channel has been studied in the present work. The aim of this paper is to find the effect of thermal conductivity of PCB, Reynolds number, spacing of the heat sources, and the effect of the emissivity of heat sources.

2. Problem geometry

The geometry considered is a three dimensional rectangular channel with six volumetric heat sources (Aluminum) protruded on a PCB and all the heat sources have the same dimensions as shown in Figure 1. Each heat source is $10.1 \times 7.5 \times 1.72$ mm, the channel has dimensions of $100 \times 50 \times 8$ mm and the substrate is 2 mm thick. The side walls and top and bottom walls are adiabatic. Air is introduced into the channel in the positive x direction at a uniform velocity u_o , and temperature, T_o . Three dimensional steady laminar incompressible flow with constant thermo-physical properties under the Boussinesq approximation is considered.

3. Grid independence study

All numerical simulations have been done using FLUENT 14.5. Figure 2 shows the results of grid independence study for of the geometry. After grid independence study, all numerical simulations were done using 3D non-uniform mesh with 2,36,946 nodes (finest). The computational mesh was more concentrated near the solid fluid interface due to larger gradients of primitive variables in these regions. A high performance computing (Virgo cluster of IIT Madras) with serial processing has been used for running the case and data files.

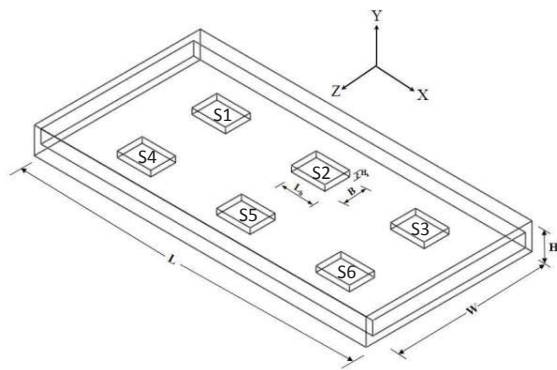


Figure 1. Isometric view of geometry.

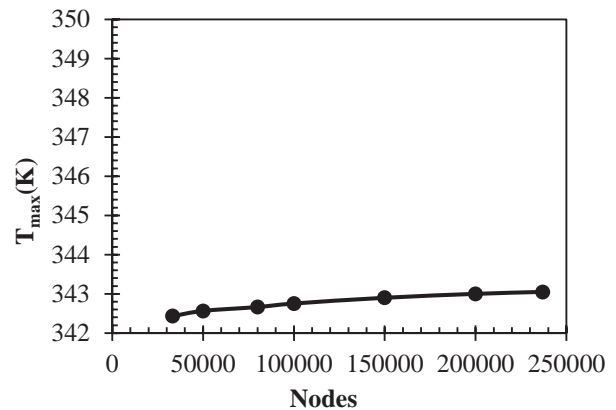


Figure 2. The effect of grid refinement on the temperature (on S3) for gap = 20 mm, $k_s = 0.038$ W/mK, $Re = 460$.

4. Governing equations

The governing equations describing the flow are conservation of mass, conservation of momentum, and the conservation of energy given by following.

Conservation of mass:

$$\frac{\partial u}{\partial x} + \frac{\partial v}{\partial y} + \frac{\partial w}{\partial z} = 0 \quad (1)$$

Conservation of momentum:

$$u \frac{\partial u}{\partial x} + v \frac{\partial u}{\partial y} + w \frac{\partial u}{\partial z} = -\frac{1}{\rho} \frac{\partial p}{\partial x} + \nu \left(\frac{\partial^2 u}{\partial x^2} + \frac{\partial^2 u}{\partial y^2} + \frac{\partial^2 u}{\partial z^2} \right) \quad (2)$$

$$u \frac{\partial v}{\partial x} + v \frac{\partial v}{\partial y} + w \frac{\partial v}{\partial z} = -\frac{1}{\rho} \frac{\partial p}{\partial y} + \nu \left(\frac{\partial^2 v}{\partial x^2} + \frac{\partial^2 v}{\partial y^2} + \frac{\partial^2 v}{\partial z^2} \right) + g\beta(T - T_o) \quad (3)$$

$$u \frac{\partial w}{\partial x} + v \frac{\partial w}{\partial y} + w \frac{\partial w}{\partial z} = -\frac{1}{\rho} \frac{\partial p}{\partial z} + \nu \left(\frac{\partial^2 w}{\partial x^2} + \frac{\partial^2 w}{\partial y^2} + \frac{\partial^2 w}{\partial z^2} \right) \quad (4)$$

Conservation of energy:

$$u \frac{\partial T}{\partial x} + v \frac{\partial T}{\partial y} + w \frac{\partial T}{\partial z} = \alpha \left(\frac{\partial^2 T}{\partial x^2} + \frac{\partial^2 T}{\partial y^2} + \frac{\partial^2 T}{\partial z^2} \right) + \frac{\alpha q'''}{k_s} \quad (5)$$

where q''' is volumetric heat generation and is zero in fluid region. In the solid region, the velocities are zero in the energy equation so that only conduction takes place.

All the surfaces of the enclosure are insulated and no slip boundary conditions are applied at the walls. Thus the boundary condition can be written as

For the top and bottom walls:

$$0 < x < L; y = 0; u = v = w = 0; \partial T / \partial y = 0$$

$$0 < x < L; y = H; u = v = w = 0; \partial T / \partial y = 0$$

And for the rest of two walls:

$$0 < x < L; z = 0; u = v = w = 0; \partial T / \partial y = 0$$

$$0 < x < L; z = 0; u = v = w = 0; \partial T / \partial y = 0$$

FLUENT is a finite volume based method, which solves the governing equations using Cartesian spatial coordinates and velocity components. Here COUPLED scheme is used for the pressure velocity coupling, and the second order upwind is used for the momentum and energy equations. Due to non-linearity of momentum equation, under relaxation is used to prevent instability and divergence.

Here all the surfaces are considered as opaque, air is considered as a non-participating medium and surface to surface model is used for solving the radiative heat flux which are calculated as given below.

For surface k

$$q_{out,k}'' = \varepsilon_k \sigma T_k^4 + (1 - \varepsilon_k) \sum_{j=1}^N F_{k,j} q_{out,j}'' \quad \text{where } j = 1, 2, 3, \dots, N \quad (6)$$

which can be written as

$$J_k = E_k + (1 - \varepsilon_k) \sum_{j=1}^N F_{k,j} J_j \quad (7)$$

For solution procedure and for more detail on equations (6) and (7) refer to ANSYS Fluent tutorial manual.

5. Validation

The results of the numerical model used in the present study is validated with the experimental data of Hotta et al. [1]. From figure 3 it appears that data the available from [1] and the present study are in good agreement.

$$(T_{max})_{excess} = T_{max} - T_o$$

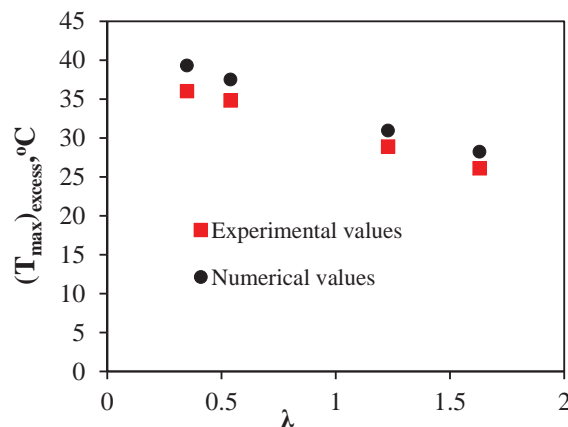


Figure 3. Variation of maximum excess temperature with different configuration.

λ – Non-dimensional distance parameter defined in [1].

6. Results and discussion

The geometry considered here is symmetric, i.e., the heat sources S1, S2 and S3 are just mirror images of the of the heat sources S4, S5, and S6. Hence, for saving the computational time, simulations have been

done for only one half of the channel (with symmetry boundary condition) for without radiation and since Fluent does not allow symmetry condition for the surface to surface radiation model and hence whole geometry has been considered for computations with surface radiation. The heat generation rate for each source is 0.2 W ($1.53 \times 10^6 \text{ W/m}^3$).

Table 1: Range of Re with corresponding Ri.

Re	115	230	345	460	575	690
Ri	11.95	2.98	1.32	0.747	0.48	0.33

Table 1 shows the Re and Ri values used in the present study. A Ri of order 1 indicates that the buoyancy forces and inertial forces are comparable to each other, leading to perfect mixed convection. For small Ri inertial forces dominate over the buoyancy forces resulting in forced convection dominating mixed convection. For high Ri buoyancy forces dominate the inertial forces resulting natural convection dominating mixed convection.

Figure 4 shows the the maximum temperature variation (i.e. on S3 and S6) for the gap = 20 mm for different k_s and for different ϵ values. It is observed that with increase in the thermal conductivity of PCB and ϵ , maximum temperature decreases considerably. Decrease in temperature with an increase in k_s means conduction within the PCB contributes considerably to the heat transfer. For each k_s value maximum temperature decreases with increase in ϵ and Reynolds number. This drop in temperature is higher at higher value of ϵ , for example at $Re = 115$, there is 3.47% reduction in temperature for $\epsilon=0.9$ while it is 1.15% for $\epsilon=0.1$. It is also observed that, at lower value of Re temperature drop is higher and this drop in temperature decreases with increase in k_s value. Also, as temperature decreases, even at the higher values of ϵ temperature drop is negligible (clearly seen in figure 4b), its means that at lower temperatures radiation contribution is low.

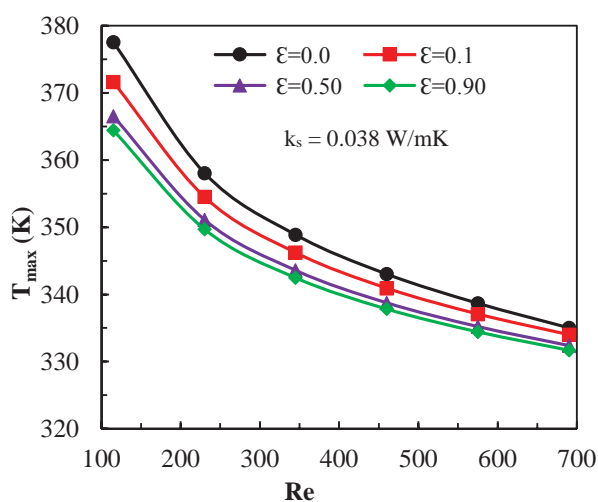


Figure 4a $k_s = 0.038 \text{ W/mK}$

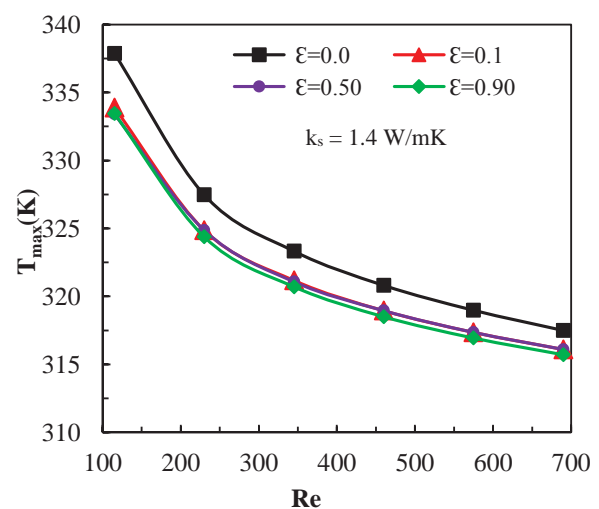


Figure 4b $k_s = 1.4 \text{ W/mK}$

Figure 4. Variation of temperature (on S3) with Re. Gap = 20 mm.

Figure 5 shows the variation of maximum temperature on each heat source, for a constant value of Re and k_s . Heat source S3 is hotter than S2 which is hotter than S1, for a given Re, the temperature of the fluid

increases along the flow direction because of heat pick up from the sources it has flowed past. There is considerable drop in temperature with increase in ϵ for each heat source.

From figure 6 it is observed that with increase in gap between the heat sources, there is a decrease in maximum temperature for each value of Re and ϵ . There is 2.23% drop of temperature for $Re = 230$ and $\epsilon = 0$ when gap increases from 5 mm to 20 mm. Also there is 4.76% drop of temperature when Re changes for 230 to 345 with gap = 5 mm and $\epsilon = 0$.

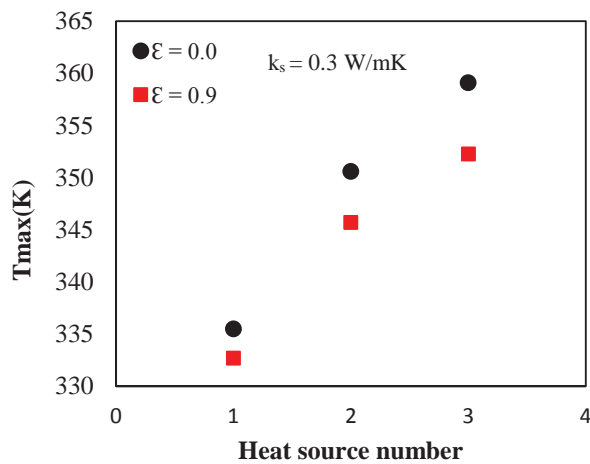


Figure 5. Variation of maximum temperature with gap = 5 mm and $Re = 115$

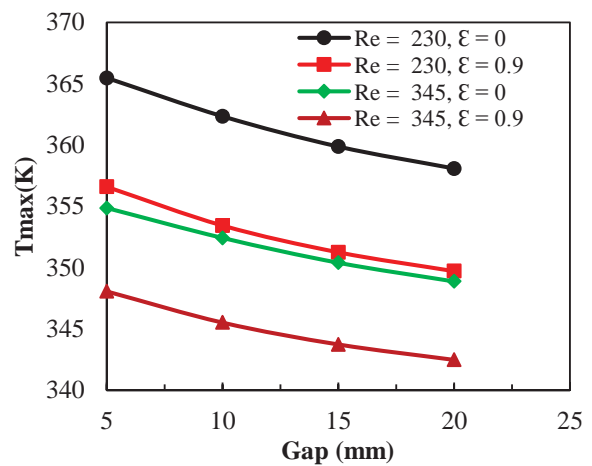


Figure 6. Temperature on S3 versus gap, for different Re at $ks = 0.038$ W/mK.

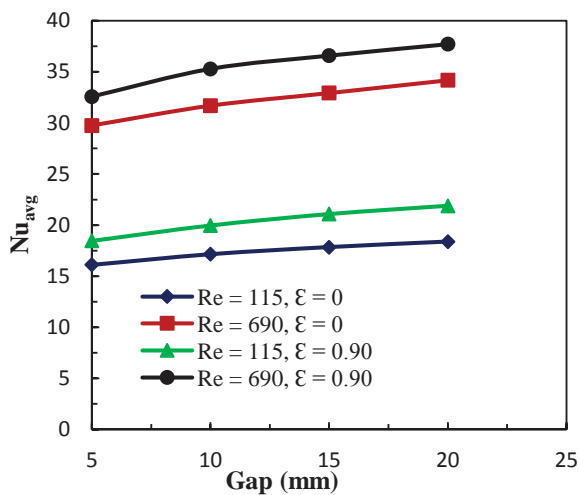


Figure 7. Nu variation with gap for different Re , on heat source S2.

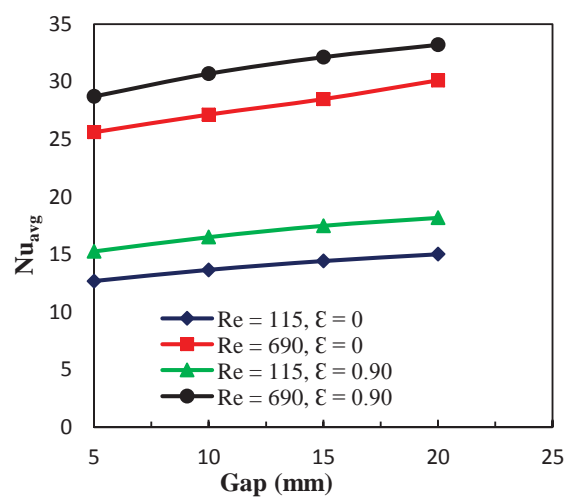


Figure 8. Nu variation with gap for different Re , on heat source S3.

Figures 7 and 8 show the distribution of the average Nusselt number on top surfaces of the source S2 and S3 respectively.

Here the Nu_{avg} is defined as

$$\text{Nu}_{\text{avg}} = \frac{h_{\text{avg}} L_h}{k_{\text{air}}} \quad \text{where} \quad h_{\text{avg}} = \frac{q}{A_{\text{sur}}(T_{\text{sur}} - T_b)}$$

The results show that the average Nusselt number on the top surface of S2 is slightly higher than that on S3 for the same Re and also with increase in ϵ , Nu increases. As the Nusselt number is proportional to the heat transfer coefficient for a given T_b , the higher the Nusselt number, the higher will be the heat dissipation. And it can be seen from these figures that the average Nusselt number increases with the increase in the spacing and also increases with increases with ϵ . As expected, there is increase in Nu with increase in Re.

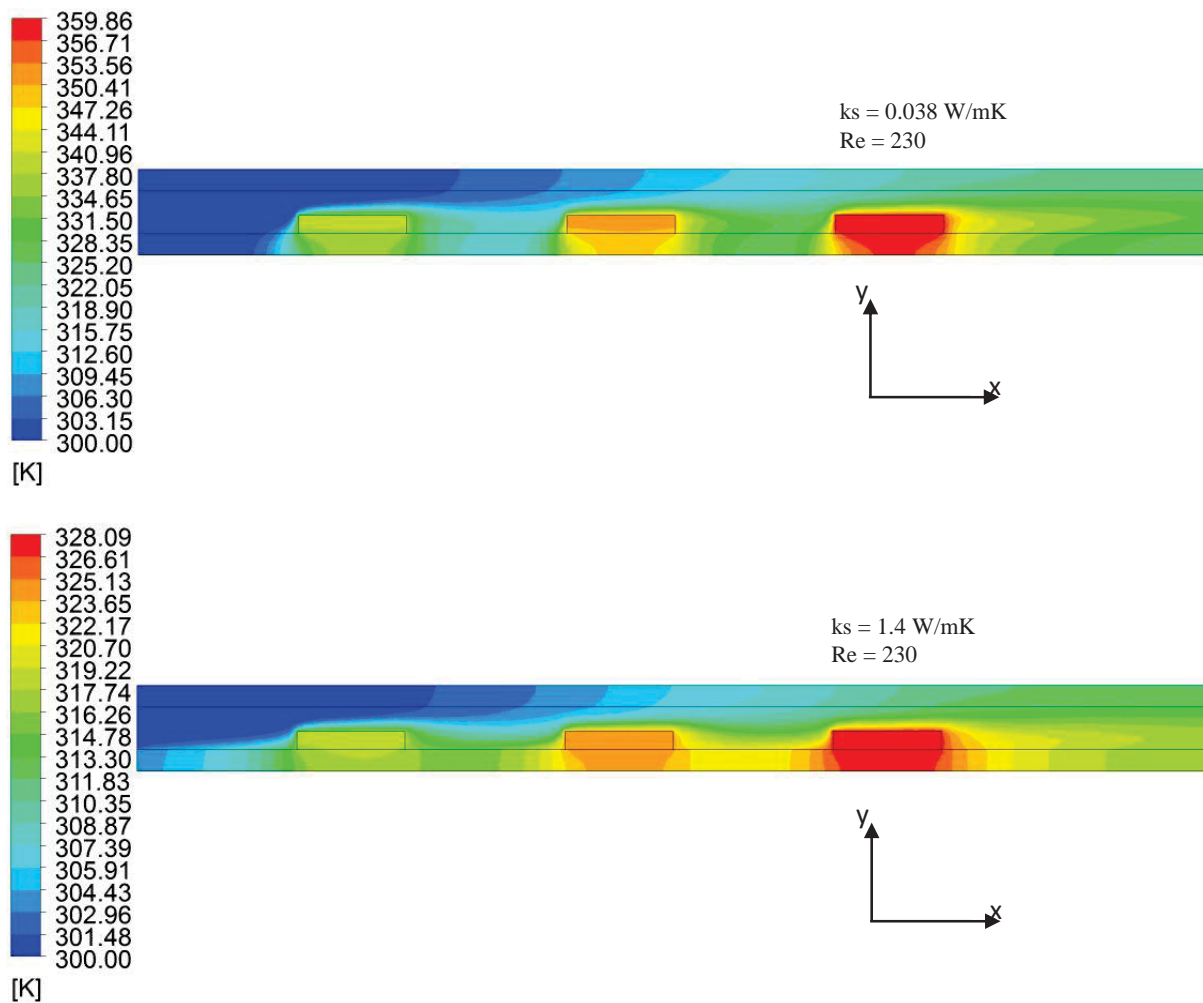


Figure 9. Temperature contour plane for different thermal conductivities of PCB. Gap = 15 mm

Figure 9 shows the temperature contours across the vertical plane passing through the middle of the heat sources for different conductivities of PCB. With increase in k_s from 0.038 to 1.4 W/mK there is a drastic reduction in maximum temperature of heat sources due to the contribution of heat conduction within the PCB.

7. Conclusions

3-Dimensional mixed convection over six heat sources (three heat sources in-line in each of the two rows) mounted on a PCB has been numerically investigated, for the Reynolds number varying from 115 to 690 and emissivity varying from 0.1 to 0.9, and for $Pr = 0.707$. The results show that the temperatures of heat sources decrease with the increase in inlet velocity. For example, there is a 11.26% drop in maximum temperature at $\mathcal{E} = 0$ and $Re = 115$. There is a 3.46% decrease in maximum temperature as \mathcal{E} changes from 0.0 to 0.9 for $Re = 115$ and $k_s = 0.038$. The heat source temperature decreases with increase in heat source gap, thermal conductivity of PCB. With the increase in Re and k_s the contribution of radiation decreases.

8. Nomenclature

A_C	Channel cross-sectional area, m^2
A_{sur}	Surface area of heat sources, m^2
c_p	Specific heat, kJ/kgK
D_h	Channel hydraulic diameter, $4A_C/P$, m
g	Gravitational acceleration, m/s^2
T_{sur}	Surface temperature of heat source, K
d	Lateral spacing between heat sources, m
k_s	Thermal conductivity of PCB, W/mK
k_{air}	Thermal conductivity of air, W/mk
P	Perimeter, m
Pr	Prandtl number
S	Heat source
q	Heat source power, W
q''	Heat flux, W/m^2K
$F_{k,j}$	View factor from k^{th} surface to j^{th} surface of an enclosure
J	Radiosity, W/m^2
Nu_{avg}	Average Nusselt number
h_{avg}	Average convection coefficient W/m^2

L_h	Length of heater, m
L	Length of channel, m
$T_{avg, e}$	Exit average temperature, K
T_b	Bulk mean temperature, K , $T_b = (T_o + T_{avg, e})/2$
T_o	Inlet temperature, K
u_o	Inlet velocity, m/s
Re_{Dh}	Reynolds number, $Re_{Dh} = (u_o D_h) / \nu_{air}$
Gr	Grashof number, $(g\beta q'' D_h^5) / (k_{air} \nu^2)$
Ri	Richardson number, Gr/Re^2

Greek symbols

β	Volumetric thermal expansion coefficient, $1/T_o$
μ	Dynamic viscosity, kg/ms
ν	Kinematic viscosity, m^2/s
\mathcal{E}	Emissivity of heat source
σ	Stefan-Boltzmann constant

9. References

- [1] Hotta T K, Balaji C and Venkateshan S P 2014 *J. of Heat Transfer* **136**/104503-5
- [2] Premachandran B and Balaji C 2006 *Int. J. of Heat and Mass Transfer* **49** 3568-82
- [3] Sawant S M and Rao C G 2008 *Heat Mass Transfer* **44** 1485-95
- [4] Yusoff S, Senoh M, Mohamed M, Ahmad K A, Abdullah M Z, Mujeebu M A, Ali M Z, Idrus F and Yaakob Y 2009 *Int. Communication in Heat and Mass Transfer*. **36** 813-19
- [5] Dogan A, Sivrioglu M and Baskaya A 2006 *Int. J. of Heat and Mass Transfer* **49** 2652-62
- [6] Choi C Y and Kim S J 1996 *Int. J. Heat Mass Transfer* **39** 1223-34
- [7] Basak T, Roy S, Sharma P K and Pop I 2009 *Int. J. of Thermal Science* **48** 891-12
- [8] Sugavanam R, Ortega A and Choi C Y 1995 *Int. J. Heat Mass Transfer* **38** 2969-84
- [9] Aminossadati S M and Ghasemi B 2009 *European J. of Mechanics B/Fluids*. **28** 590-598